

# Robust Tracking Control For Uncertain Neural Network Dynamics Models

Xiao Li

Yutong Li

Anouck Girard

Ilya Kolmanovsky

*University of Michigan, Ann Arbor, MI, USA*

HSIAOLI@UMICH.EDU

YUTLI@UMICH.EDU

ANOUCK@UMICH.EDU

ILYA@UMICH.EDU

## Abstract

The Neural Network (NN), as a black-box function approximator, has been considered in many control applications. However, the difficulties in verifying the overall system safety, in the presence of uncertainties, hinder the deployment of NN in safety-critical systems. In this paper, we consider an NN-learned dynamic model that imitates an unknown real-world dynamical system and is subject to both bounded intrinsic and extrinsic uncertainties. We leverage the learned NN dynamic model to control the actual dynamical system. In this setting, we formulate the constrained reference tracking problem and show that it can be solved using Mixed-integer Linear Programming (MILP). The proposed MILP-based solution enjoys a provable safety guarantee, and these properties are also empirically demonstrated in navigating robots and avoiding obstacles in simulations.

**Keywords:** neural networks, safety-critical systems, uncertainties, trajectory tracking

## 1. Introduction

The Neural Networks, as universal function approximators (Hornik et al. (1989)), have been extensively utilized to learn latent input-to-output mappings from data. For instance, many robotics applications deploy NNs compute paths for autonomous vehicles (Barnes et al. (2017)) from input camera images, and imitate the vehicle dynamics (Wei and Liu (2021)). However, the NNs, as approximators of the actual mappings, have errors. In safety-critical control applications, including those leveraging NNs as control-oriented predictive models of the underlying actual dynamics, there are also other (extrinsic) sources of uncertainty such as neglected actuator dynamics and sense measurement noise (see Figure 1). In this work, we consider both intrinsic and extrinsic uncertainties and assume that these uncertainties are set-bounded.

Much research has been pursued to develop formal safety guarantees. The methods based on the Control Barrier Function (CBF) have been investigated to synthesize barrier functions to enforce safety constraints (Wang et al. (2018); Dai et al. (2017)). The CBFs have also been utilized to avoid collision in robotic systems with NN-learned dynamics (Wei and Liu (2021)) and with perception module (Tong et al. (2023)). However, the notion of uncertainties has not been considered in the literature above. Probabilistic (Berkenkamp et al. (2016)) and set-membership-based methods (Aswani et al. (2013)) have been previously considered to handle the uncertainties in nonlinear dynamic models. Probabilistic methods have also been investigated to train NN with prediction confidence levels (Gal and Ghahramani (2016); Lakshminarayanan et al. (2017)). The discussion of uncertainty quantification of NNs is not in the scope of this work.

Hewing et al. (2020) provides a review of techniques used to quantify and incorporate model uncertainties in control implementation. The robust controllers have been developed which account

for the derived bounds on perception errors (Dean et al. (2020, 2021); Dean and Recht (2021)). Differently from the existing literature, we focus on exploiting the structure of NNs in accounting for the uncertainty propagation where the NN serves as a predictive model of the latent dynamics. Mixed Integer Programming (MIP) (Tjeng et al. (2017)) and Semi-Definite Programming (SDP) (Hu et al. (2020)) have been used to assess the robustness of NN-based solutions. Unlike Tjeng et al. (2017) and Hu et al. (2020), we consider the setting in which the NN inputs are affected by uncertainties which belong to a set that depends on the decision variable. This setting is relevant to applications using control-oriented NN predictive models.

The contributions of this paper are as follows: 1) We propose an approach leveraging an NN-learned dynamic model for robust reference tracking subject to constraints. The safety and dynamics constraints are informed by uncertainty set propagation through the NN and are handled by MILP. 2) We consider both intrinsic uncertainties from NN prediction errors and extrinsic uncertainties present in the actual system, and establish theoretical safety guarantees for the proposed method. 3) The theoretical properties are further demonstrated in simulations of navigating omnidirectional robots and vehicles which ensuring collision avoidance.

This paper is organized as follows: In Section 2, we introduce the assumptions on the actual dynamical system and NN learned ones, and we formulate the robust tracking problem. In Section 3, we present our method using MILP and its theoretical properties. In Section 4, we use the proposed method, in combination with a Reachability-Guided RRT algorithm, to navigate a mass-point omnidirectional robot through a maze filled with obstacles. In Section 5, we leverage a set-theoretical localization algorithm that provides vehicle state measurement with uncertainty bounds, and we use our method to navigate a vehicle while avoiding collisions. Finally, the conclusions are given in Section 6 and the proofs of the theoretical properties are presented in Appendix A.

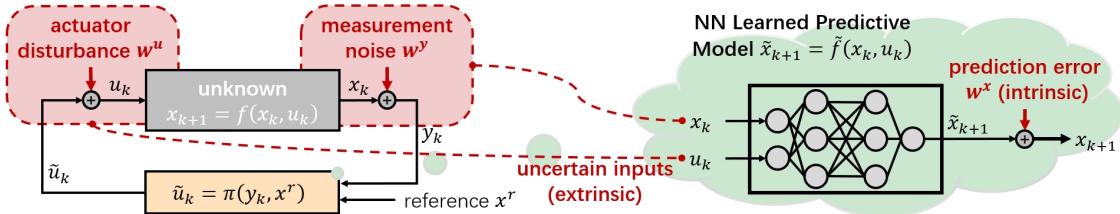


Figure 1: Robust tracking of unknown dynamics using an NN learned predictive model considering intrinsic and extrinsic uncertainties (labeled in red fonts).

## 2. Problem Formulation

We consider a discrete-time dynamic system represented by  $x_{k+1} = f(x_k, u_k)$ , where  $x_k \in \mathcal{X}$  is the state vector and  $\mathcal{X} \subset \mathbb{R}^{n_x}$  is the state feasible set;  $u_k \in \mathcal{U}$  is the control and  $\mathcal{U} \subset \mathbb{R}^{n_u}$  is the control admissible set; and  $f : \mathcal{X} \times \mathcal{U} \rightarrow \mathcal{X}$  is an unknown nonlinear mapping. In the sequel, we use lowercase letters, e.g.,  $x, y, u, w$ , to represent vectors, capital letters, e.g.,  $W$ , to define matrices, and scripted letters, e.g.,  $\mathcal{X}, \mathcal{U}$ , to denote sets. We first discuss the neural network learned dynamic model for controller design that is subject to both intrinsic and extrinsic uncertainties in Section 2.1. Then, we introduce the robust tracking problem ensuring safety under uncertainties in Section 2.2.

## 2.1. Model Preliminaries

As shown in Figure 1, we approximate the dynamics  $f$  with a pre-trained  $\ell$ -layer fully connected neural network (NN)  $\tilde{f} : \mathcal{X} \times \mathcal{U} \rightarrow \mathcal{X}$  that admits the following form

$$\begin{aligned} z_i &= \sigma^{(i)}(\hat{z}_i), \quad \hat{z}_i = W^{(i)} z_{i-1} + b^{(i)}, \quad i = 1, \dots, \ell - 1, \\ z_0 &= [x_k^T, u_k^T]^T, \quad \tilde{x}_{k+1} = W^{(\ell)} z_{\ell-1} + b^{(\ell)}, \end{aligned} \quad (1)$$

where  $W^{(i)} \in \mathbb{R}^{n_i \times n_{i-1}}$ ,  $b^{(i)} \in \mathbb{R}^{n_i}$  and  $\sigma^{(i)} : \mathbb{R}^{n_i} \rightarrow \mathbb{R}^{n_i}$  are the weight matrix, the bias vector and an element-wise nonlinear activation function in the  $i^{th}$  layer, respectively. The NN uses the inputs  $x_k, u_k$  to compute a prediction  $\tilde{x}_{k+1} = \tilde{f}(x_k, u_k)$  of the actual state  $x_{k+1}$ . We consider the NN-learned dynamic model to be subject to uncertainties (see Figure 1) of three types: The NN prediction  $\tilde{x}_{k+1}$  of the actual state  $x_{k+1}$  is subject to an unknown prediction error  $w_k^x$ , i.e.,

$$\tilde{x}_{k+1} = x_{k+1} + w_k^x, \quad w_k^x \in \mathcal{W}_x, \quad (2)$$

where  $\mathcal{W}_x \subset \mathbb{R}^{n_x}$  is a bounded set; Moreover, we suppose that the actual states  $x_k$  and the actual control input  $u_k$  are latent due to the presents of noises. However, we assume that a state measurement  $y_k$  of the actual state  $x_k$  is available and admits the following form

$$y_k = x_k + w_k^y, \quad w_k^y \in \mathcal{W}_y, \quad (3)$$

where  $w_k^y$  is an unknown measurement noise, and  $\mathcal{W}_y \subset \mathbb{R}^{n_x}$  is a bounded set; Meanwhile, we design a feedback controller  $\pi : \mathcal{X} \times \mathcal{X} \rightarrow \mathcal{U}$  to track the reference state  $x^r$  and the actual control signal  $u_k$  is subject to an unknown additive actuator disturbance  $w_k^u$ , i.e.,

$$u_k = \tilde{u}_k + w_k^u, \quad \tilde{u}_k = \pi(y_k, x^r), \quad w_k^u \in \mathcal{W}_u, \quad (4)$$

where  $\mathcal{W}_u \subset \mathbb{R}^{n_u}$  is a bounded set.

## 2.2. Robust Constrained Tracking Problem

Suppose there exists an unsafe subset  $\mathcal{X}_u \subset \mathcal{X}$ , e.g., obstacles, that the system should avoid. Given a reference  $x^r \in \mathcal{X}_s$  in the safe complement subset  $\mathcal{X}_s = \mathcal{X} \setminus \mathcal{X}_u$  and a state measurement  $y_k$  that obeys the assumption in (3), our task is to design a controller  $\pi(y_k, x^r)$  to track the reference  $x^r$  while keeping the system in the safe subset  $\mathcal{X}_s$ , i.e., ensuring  $x_{k+1} \in \mathcal{X}_s$  given  $x_k \in \mathcal{X}_s$ . These objectives can be accounted for by a constrained optimization problem,

$$\pi(y_k, x^r) = \underset{\tilde{u}_k}{\operatorname{argmin}} \left( \max_{x \in \mathcal{F}(\mathcal{X}_k, \mathcal{U}_k(\tilde{u}_k))} \|x - x^r\|_p \right) \quad (5a)$$

$$\text{subject to:} \quad \tilde{u}_k \in \mathcal{U}, \quad \mathcal{X}_k = (y_k \ominus \mathcal{W}_y) \cap \mathcal{X}_s, \quad \mathcal{U}_k = \mathcal{U}_k(\tilde{u}_k) = (\tilde{u}_k \oplus \mathcal{W}_u) \cap \mathcal{U}, \quad (5b)$$

$$\tilde{\mathcal{F}}(\mathcal{X}_k, \mathcal{U}_k) = \left\{ \tilde{x}_{k+1} \in \mathcal{X} : \tilde{x}_{k+1} = \tilde{f}(x_k, u_k), \forall x_k \in \mathcal{X}_k, u_k \in \mathcal{U}_k \right\}, \quad (5c)$$

$$\mathcal{F}(\mathcal{X}_k, \mathcal{U}_k) = \tilde{\mathcal{F}}(\mathcal{X}_k, \mathcal{U}_k) \oplus \mathcal{W}_x, \quad \mathcal{F}(\mathcal{X}_k, \mathcal{U}_k) \subset \mathcal{X}_s, \quad (5d)$$

where  $\tilde{u}$  is the decision variable,  $\|\cdot\|_p$  represents the  $\ell_p$  norm (we consider  $p = 1$  in the sequel),  $\ominus$  represents the Pontryagin difference, and  $\oplus$  denotes the Minkowski sum. The term  $y_k \ominus \mathcal{W}_y$  stands for  $\{y_k\} \ominus \mathcal{W}_y$  where we omit the curly brackets for simplicity. Given the measurement  $y_k$  that satisfies (3), the set  $\mathcal{X}_k$  in constraint (5b) represents an uncertainty set that contains the actual state  $x_k$ . Similarly, the set  $\mathcal{U}_k$  in constraint (5b) depends on the decision variable  $\tilde{u}_k$  and contains the

actual control  $u_k$  based on (4). The set-valued function  $\tilde{\mathcal{F}} : \mathcal{X} \times \mathcal{U} \rightarrow \mathcal{X}$  in (5c) calculates the one step ahead reachable set of the learned NN dynamic model. The reachable set  $\mathcal{F}(\mathcal{X}_k, \mathcal{U}_k)$  in (5d) is derived from  $\tilde{\mathcal{F}}(\mathcal{X}_k, \mathcal{U}_k)$  and contains the actual state  $x_{k+1}$  based on (2). Meanwhile, the constraints in (5d) also guarantee the safety of the next state  $x_{k+1}$  for all the possible uncertainties modeled by (2), (3), (4). The objective defined by (5a) minimizes the maximum distance between the states in the reachable set  $\mathcal{F}(\mathcal{X}_k, \mathcal{U}_k)$  and the reference, thereby steering the system closer to  $x^r$ . Note that the input set  $\mathcal{U}_k = \mathcal{U}_k(\tilde{u}_k)$  is conditioned on the decision variable  $\tilde{u}_k$ .

### 3. Mixed-integer Linear Programming

To simplify the exposition of the approach, we assume the uncertainty sets in (2), (3), (4) are hyper-cubes defined according to

$$\mathcal{W}_x = \{w^x \in \mathbb{R}^{n_x} : |w^x| \leq \epsilon^x, \epsilon^x \in \mathbb{R}^{n_x}, \epsilon^x \geq 0\}, \quad (6a)$$

$$\mathcal{W}_y = \{w^y \in \mathbb{R}^{n_x} : |w^y| \leq \epsilon^y, \epsilon^y \in \mathbb{R}^{n_x}, \epsilon^y \geq 0\}, \quad (6b)$$

$$\mathcal{W}_u = \{w^u \in \mathbb{R}^{n_u} : |w^u| \leq \epsilon^u, \epsilon^u \in \mathbb{R}^{n_u}, \epsilon^u \geq 0\}. \quad (6c)$$

Note tat, in principle, one can always find a hypercube overbounding a bounded set. Moreover, we assume the nonlinear functions in the NN model are ReLU activation functions

$$\sigma^{(i)}(x) = \text{ReLU}(x) = \max\{0, x\}, \quad i = 1, \dots, \ell, \quad (7)$$

which are commonly adopted in different NN architectures and have good empirical performance (LeCun et al. (2015).) With a little abuse of notation, we use  $a \leq b$  to denote the element-wise order between two vectors  $a, b \in \mathbb{R}^n$ . In the sequel, given a lower bound  $a \in \mathbb{R}^n$ , an upper bound  $b \in \mathbb{R}^n$  and  $a \leq b$ , we use  $[a, b]$  to denote a hypercube in  $\mathbb{R}^n$ . We use  $I_{n \times n}$  to represent the identity matrix of size  $n$ . We use  $\mathbb{1}_{n \times m}$ , and  $\mathbb{0}_{n \times m}$  to denote a matrix with all zeros and ones, respectively, of size  $n \times m$ . We neglect the subscript  $n \times m$  in calculations assuming that the dimensions are appropriate. Meanwhile, we consider the state feasible set, control admissible set, and unsafe set according to

$$\mathcal{X} = [\underline{x}, \bar{x}], \quad \underline{x}, \bar{x} \in \mathbb{R}^{n_x}, \quad \underline{x} \leq \bar{x}, \quad (8a)$$

$$\mathcal{U} = [\underline{u}, \bar{u}], \quad \underline{u}, \bar{u} \in \mathbb{R}^{n_u}, \quad \underline{u} \leq \bar{u}, \quad (8b)$$

$$\mathcal{X}_u = \cup_i \mathcal{X}_u^{(i)}, \quad \mathcal{X}_u^{(i)} = [\underline{x}_u^{(i)}, \bar{x}_u^{(i)}], \quad \underline{x}_u^{(i)}, \bar{x}_u^{(i)} \in \mathbb{R}^{n_x}, \quad \underline{x} \leq \underline{x}_u^{(i)} \leq \bar{x}_u^{(i)} \leq \bar{x}. \quad (8c)$$

The definition of the unsafe set (8c) enables us to tightly over-bound obstacles of irregular shapes using unions of hypercubes in the optimization problem. Then, the equations (5b), (5c), (5d) encode the constraints associated with the input feasibility, NN structural non-linearity, and system safety, respectively, and are realized using integer decision variables as described in the respective Sections 3.1, 3.2, and 3.3. We also focus on the case when  $p = 1$  in (5a), i.e., the cost function is based on  $\ell_1$  norm which leads to a MILP in Section 3.4. We prove that the formulated optimization constraints in this section can guarantee safety in Appendix A.

#### 3.1. Constraints Embedding Input Feasibility

Given a measurement  $y_k$  and the decision variable  $\tilde{u}_k$ , the constraints (5b) define the sets  $\mathcal{X}_k$ ,  $\mathcal{U}_k$  that guarantee to contain the actual state  $x_k$  and the control  $u_k$  while the decision variable shall be admissible, i.e.,  $x_k \in \mathcal{X}_k$ ,  $u_k \in \mathcal{U}_k$ ,  $\tilde{u}_k \in \mathcal{U}_k$ . We embed these feasibility conditions of the NN inputs using linear inequality and equality constraints in the following proposition.

**Proposition 1** *Given state measurement  $y_k$  and a decision variable  $\tilde{u}_k$ , suppose the unknown actual quantities  $x_k$  and  $u_k$  obey (3), (4) with assumptions in (6b), (6c), (8a), (8b). Let the decision variables  $\tilde{u}_k \in \mathbb{R}^{n_u}$ ,  $a_0, b_0 \in \mathbb{R}^{n_x+n_u}$ , and  $\delta^a, \delta^b \in \mathbb{R}^{n_u}$  satisfy the following constraints*

$$a_{0,1:n_x} = \max\{\underline{x}, y_k - \epsilon^y\}, \quad b_{0,1:n_x} = \min\{\bar{x}, y_k + \epsilon^y\}, \quad a_0 \leq b_0, \quad (9)$$

$$\begin{aligned} & \underline{u} \leq \tilde{u}_k \leq \bar{u}, \quad \delta_j^a, \delta_j^b \in \{0, 1\}, \quad j = 1, \dots, n_u, \\ & \begin{cases} a_{0,(n_x+1):(n_x+n_u)} \geq \underline{u} \\ a_{0,(n_x+1):(n_x+n_u)} \geq \tilde{u}_k - \epsilon^u \\ a_{0,(n_x+1):(n_x+n_u)} \leq \underline{u} + M(\mathbb{1} - \delta^a) \\ a_{0,(n_x+1):(n_x+n_u)} \leq \tilde{u}_k - \epsilon^u + M\delta^a \end{cases}, \quad \begin{cases} b_{0,(n_x+1):(n_x+n_u)} \leq \bar{u} \\ b_{0,(n_x+1):(n_x+n_u)} \leq \tilde{u}_k + \epsilon^u \\ b_{0,(n_x+1):(n_x+n_u)} \geq \bar{u} - M(\mathbb{1} - \delta^b) \\ b_{0,(n_x+1):(n_x+n_u)} \geq \tilde{u}_k + \epsilon^u - M\delta^b \end{cases}, \end{aligned} \quad (10)$$

where  $\delta_j^a$  denotes the  $j$ th element in column vector  $\delta^a$ ,  $a_{0,m:n}$  represents the vector containing elements between row  $n$  and row  $m$  in  $a_0$ , the constant matrix  $M = \text{Diag}(\max\{\epsilon^u, \bar{u} - \underline{u} - \epsilon^u\})$ , and  $\text{Diag}(x) \in \mathbb{R}^{n \times n}$  yields a square matrix with elements of  $x$  on the diagonal and zero anywhere else. Then, it's guaranteed that  $z_0 = [x_k^T \ u_k^T]^T \in [a_0, b_0]$ .

The constraints in Proposition 1 enforce input feasibility, i.e.,  $\tilde{u}_k \in \mathcal{U}_k$ , and provide bounds  $a_0, b_0$  to the NN input subject to extrinsic uncertainties, i.e.,  $a_0 \leq [x^T, u^T]^T \leq b_0$  for all  $x \in \mathcal{X}_k$ ,  $u \in \mathcal{U}_k$ . Specifically, based on assumption (6b) and (8a), the constraints (9) imply  $\mathcal{X}_k \subseteq [a_{0,1:n_x}, b_{0,1:n_x}]$ . Based on assumption (6c) and (8b), the constraints (10) are equivalent to the following inequalities

$$\max\{\underline{u}, \tilde{u}_k - \epsilon^u\} = a_{0,(n_x+1) \dots (n_x+n_u)} \leq b_{0,(n_x+1) \dots (n_x+n_u)} = \min\{\bar{u}, \tilde{u}_k + \epsilon^u\},$$

thereby we have  $\mathcal{U}_k \subseteq [a_{0,(n_x+1):(n_x+n_u)}, b_{0,(n_x+1):(n_x+n_u)}]$ . We introduce the integer variables  $\delta^a, \delta^b$  to move the decision variable  $\tilde{u}_k$  out of the nonlinear min/max function:  $\delta_j^a = 1$  implies the  $j$ th element of  $\max\{\underline{u}, \tilde{u}_k - \epsilon^u\}$  attains the value of  $j$ th element of  $\underline{u}$ , otherwise  $\delta_j^a = 0$ ;  $\delta_j^b = 1$  indicates the  $j$ th element of  $\min\{\bar{u}, \tilde{u}_k + \epsilon^u\}$  attains the value of  $j$ th element of  $\bar{u}$ , otherwise  $\delta_j^b = 0$ . The proof is presented in A.1.

### 3.2. Constraints Encoding NN Structural Non-Linearity

Using the bounded sets  $\mathcal{X}$  in (8a) and  $\mathcal{U}$  in (8b), we can numerically derive lower and upper bounds  $\hat{\underline{z}}_i, \hat{\bar{z}}_i \in \mathbb{R}^{n_i}, i = 1, \dots, \ell$  on the neuron values  $\hat{z}_i$  and the output  $\tilde{x}_{k+1}$  using interval arithmetic, i.e.,  $\hat{z}_i \in [\hat{\underline{z}}_i, \hat{\bar{z}}_i]$  and  $\tilde{x}_{k+1} \in [\hat{\underline{z}}_\ell, \hat{\bar{z}}_\ell]$ . In the sequel, these derived bounds are used to tighten the constraints and limit the search region for the optimization solver. Given the decision variables  $a_0, b_0$  in Proposition 1 as bounds on the NN input, we can explicitly encode the variable uncertainty set propagation through the NN defined in (5c) using the following results:

**Proposition 2** *Given  $z_0 = [x_k^T \ u_k^T]^T \in [a_0, b_0]$ , consider a NN defined by (1) and (7), and let the decision variables  $a_{i-1}, b_{i-1} \in \mathbb{R}^{n_{i-1}}$ ,  $\hat{a}_i, \hat{b}_i \in \mathbb{R}^{n_i}$ ,  $\delta_i^{--}, \delta_i^{+-}, \delta_i^{++} \in \{0, 1\}^{n_i}$ ,  $i = 1, \dots, \ell - 1$ , and  $a_{k+1}, b_{k+1} \in \mathbb{R}^{n_x}$  satisfy the following constraints*

$$\begin{aligned} \hat{a}_{i,j} &= w_j^{(i)} S_i \left( (w_j^{(i)})^T \right) \begin{bmatrix} a_{i-1} \\ b_{i-1} \end{bmatrix} + b_j^{(i)}, \quad \hat{b}_{i,j} = w_j^{(i)} S_i \left( (w_j^{(i)})^T \right) \begin{bmatrix} b_{i-1} \\ a_{i-1} \end{bmatrix} + b_j^{(i)}, \\ \hat{\underline{z}}_i &\leq \hat{a}_i \leq \hat{b}_i \leq \hat{\bar{z}}_i, \quad \forall j = 1, \dots, n_i, \quad \forall i = 1, \dots, \ell - 1, \end{aligned} \quad (11)$$

$$\begin{cases} a_i \geq \hat{a}_i \\ a_i \leq \hat{a}_i - \text{Diag}(\hat{z}_i)(\delta_i^{--} + \delta_i^{++}) \\ a_i \leq \text{Diag}(\hat{z}_i)\delta_i^{++} \end{cases}, \quad \begin{cases} b_i \geq \hat{b}_i \\ b_i \leq \hat{b}_i - \text{Diag}(\hat{z}_i)\delta_i^{--} \\ b_i \leq \text{Diag}(\hat{z}_i)(\delta_i^{--} + \delta_i^{++}) \end{cases}, \quad (12)$$

$$0 \leq a_i \leq b_i, \quad \delta_{i,j}^{--}, \delta_{i,j}^{--}, \delta_{i,j}^{++} \in \{0, 1\}, \quad \delta_{i,j}^{--} + \delta_{i,j}^{--} + \delta_{i,j}^{++} = 1, \\ \forall j = 1, \dots, n_i, \quad \forall i = 1, \dots, \ell - 1,$$

$$\begin{aligned} \hat{z}_\ell \leq a_{k+1} \leq b_{k+1} \leq \bar{z}_\ell, \quad a_{k+1,j} = w_j^{(\ell)} S_\ell \left( (w_j^{(\ell)})^T \right) \begin{bmatrix} a_{\ell-1} \\ b_{\ell-1} \end{bmatrix} + b_j^{(\ell)}, \\ b_{k+1,j} = w_j^{(\ell)} S_\ell \left( (w_j^{(\ell)})^T \right) \begin{bmatrix} b_{\ell-1} \\ a_{\ell-1} \end{bmatrix} + b_j^{(\ell)}, \quad \forall j = 1, \dots, n_i, \end{aligned} \quad (13)$$

where  $\hat{a}_{i,j}$  is the  $j^{\text{th}}$  element of  $\hat{a}_i$ ;  $w_j^{(i)}$  is the  $j^{\text{th}}$  row of  $W^{(i)}$ ;  $b_j^{(i)}$  is the  $j^{\text{th}}$  element of  $b^{(i)}$ ;  $\delta_{i,j}^{--}$  denotes the  $j^{\text{th}}$  element of  $\delta_i^{--}$ ;  $a_{k+1,j}, b_{k+1,j}$  represent the  $j^{\text{th}}$  element of  $a_{k+1}, b_{k+1}$ , respectively; The functions  $S_i : \mathbb{R}^{n_{i-1}} \rightarrow \mathbb{R}^{n_{i-1} \times 2n_{i-1}}$  and  $s : \mathbb{R} \rightarrow \mathbb{R}^{2n_{i-1}}$  are defined according to

$$S_i \left( \begin{bmatrix} \vdots \\ w_q \\ \vdots \end{bmatrix} \right) = \begin{bmatrix} \vdots \\ (s(w_q))^T \\ \vdots \end{bmatrix}, \quad s(w_q) := \begin{cases} \begin{bmatrix} e_q \\ \mathbb{0}_{n_{i-1} \times 1} \end{bmatrix} & \text{if } w_q \geq 0 \\ \begin{bmatrix} \mathbb{0}_{n_{i-1} \times 1} \\ e_q \end{bmatrix} & \text{if } w_q < 0 \end{cases},$$

and  $e_q \in \mathbb{R}^{n_{i-1}}$  ( $q = 1, \dots, n_{i-1}$ ) has 1 in the  $q^{\text{th}}$  element and zero anywhere else. Then, the variable reachable set  $\tilde{\mathcal{F}}(\mathcal{X}_k, \mathcal{U}_k)$  defined in (5c) is a subset of hypercube  $[a_{k+1}, b_{k+1}]$ , i.e.,  $\tilde{\mathcal{F}}(\mathcal{X}_k, \mathcal{U}_k) \subseteq [a_{k+1}, b_{k+1}]$ .

From  $(i-1)$ st to  $i$ th layer of the NN, the uncertainty set propagation is realized through variables  $a_{i-1}, b_{i-1}$  and  $\hat{a}_i, \hat{b}_i$  that are the lower and upper bounds of  $z_{i-1}$  and  $\hat{z}_i$ , respectively (i.e.,  $z_{i-1} \in [a_{i-1}, b_{i-1}]$  and  $\hat{z}_i \in [\hat{a}_i, \hat{b}_i]$ ). The constraints (11) and (13) encode the uncertainty propagation through the fully connected layers,  $\hat{z}_i = W^{(i)} z_{i-1} + b^{(i)}$  and  $\tilde{x}_{k+1} = W^{(\ell)} z_{\ell-1} + b^{(\ell)}$ , respectively. The uncertainty set propagation through the nonlinear ReLU function is enforced in constraints (12). In constraints (11) and (13), the  $q$ th row of matrix  $S_i((w_j^{(i)})^T)$  switches the upper and lower bounds of  $z_{i-1}$  if the  $q$ th element in  $w_j^{(i)}$  is negative. Meanwhile, since the values  $z_{i-1}$  in neurons fall into a bounded hypercube  $[a_{i-1}, b_{i-1}]$ , the activation status of each ReLU activation function is uncertain. Inspired by Tjeng et al. (2017), we introduce integer variables  $\delta_i^{--}, \delta_i^{--}, \delta_i^{++}$  in constraints (12) to encode the uncertainty in the ReLU activation status according to

$$\hat{a}_{i,j} \leq \hat{b}_{i,j} \leq 0 \text{ if } \delta_{i,j}^{--} = 1; \quad \hat{a}_{i,j} \leq 0 \leq \hat{b}_{i,j} \text{ if } \delta_{i,j}^{--} = 1; \quad 0 \leq \hat{a}_{i,j} \leq \hat{b}_{i,j} \text{ if } \delta_{i,j}^{++} = 1.$$

Furthermore, as can be shown, the hypercube defined by lower bound  $a_{k+1}$  and upper bound  $b_{k+1}$  is actually an over-estimation of the actual reachable set  $\tilde{\mathcal{F}}$ , i.e.,  $\tilde{\mathcal{F}} \subseteq [a_{k+1}, b_{k+1}]$ . The proof is presented in Appendix A.2.

### 3.3. Constraints Enforcing System Safety

Given a hypercube  $[a_{k+1}, b_{k+1}]$  as an over-estimation of the reachable set  $\tilde{\mathcal{F}}$  in Proposition 2, we enforce the safety constraints (5d) of the system such that  $x_{k+1} \in \mathcal{F}(\mathcal{X}_k, \mathcal{U}_k) \subset \mathcal{X}_s$ . We consider the presence of a simple unsafe subset  $\mathcal{X}_u = [\underline{x}_u, \bar{x}_u]$  in the following result and discuss the extension to a union of  $\mathcal{X}_u^{(i)}$  defined in (8c) at the end of this section.



**Proposition 3** Given  $\tilde{\mathcal{F}}(\mathcal{X}_k, \mathcal{U}_k) \subseteq [a_{k+1}, b_{k+1}]$  and state space defined in (8a), suppose the NN predictions are subject to bounded additive errors defined in (2) and (6a), and the decision variables  $\underline{x}_{k+1}, \bar{x}_{k+1} \in \mathbb{R}^{n_x}$ ,  $\delta_1^u, \delta_2^u \in \mathbb{R}^{n_x}$  satisfy the following constraints

$$\underline{x} \leq \underline{x}_{k+1} \leq \bar{x}_{k+1} \leq \bar{x}, \quad \underline{x}_{k+1} = a_{k+1} - \epsilon^x, \quad \bar{x}_{k+1} = b_{k+1} + \epsilon^x, \quad (14)$$

$$\begin{cases} \bar{x}_{k+1} \leq \bar{x} + \text{Diag}(\underline{x}_u - \bar{x}) \delta_1^u \\ \bar{x}_{k+1} \geq \underline{x}_u - \text{Diag}(\underline{x}_u - \underline{x}) \delta_1^u \\ \underline{x}_{k+1} \geq \underline{x} + \text{Diag}(\bar{x}_u - \underline{x}) \delta_2^u \\ \underline{x}_{k+1} \leq \bar{x}_u - \text{Diag}(\bar{x}_u - \bar{x}) \delta_2^u \end{cases}, \quad \begin{cases} \delta_{1,j}^u, \delta_{2,j}^u \in \{0, 1\}, \quad \forall j = 1, \dots, n_x, \\ \delta_{1,j}^u + \delta_{2,j}^u \leq 1, \quad \forall j = 1, \dots, n_x, \\ \sum_{j=1}^{n_x} (\delta_{1,j}^u + \delta_{2,j}^u) \geq 1, \end{cases} \quad (15)$$

where  $\delta_{1,j}^u, \delta_{2,j}^u$  are the  $j$ th element of  $\delta_1^u, \delta_2^u$ , respectively. Then,  $x_{k+1} \in \mathcal{F}(\mathcal{X}_k, \mathcal{U}_k)$  where  $\mathcal{F}(\mathcal{X}_k, \mathcal{U}_k)$  is the reachable set defined in (5d), and  $\mathcal{F}(\mathcal{X}_k, \mathcal{U}_k) \subseteq [\underline{x}_{k+1}, \bar{x}_{k+1}] \subset \mathcal{X}_s$  with  $\mathcal{X}_u = [\underline{x}_u, \bar{x}_u]$ .

In Proposition 3, the constraints (14) are equivalent to  $[\underline{x}_{k+1}, \bar{x}_{k+1}] = [a_{k+1}, b_{k+1}] \oplus \mathcal{W}_x$  and  $[\underline{x}_{k+1}, \bar{x}_{k+1}] \subset \mathcal{X}$ . Considering the result  $\tilde{\mathcal{F}}(\mathcal{X}_k, \mathcal{U}_k) \subseteq [a_{k+1}, b_{k+1}]$  from Proposition 2, it is obvious that  $\mathcal{F}(\mathcal{X}_k, \mathcal{U}_k) \subseteq [\underline{x}_{k+1}, \bar{x}_{k+1}]$  based on the definition of  $\mathcal{F}(\mathcal{X}_k, \mathcal{U}_k)$  in (5d). Subsequently, the safety constraint of  $\mathcal{F}(\mathcal{X}_k, \mathcal{U}_k) \subset \mathcal{X}_s$  can be enforced with  $[\underline{x}_{k+1}, \bar{x}_{k+1}] \subset \mathcal{X}_s$  which is equivalent to  $[\underline{x}_{k+1}, \bar{x}_{k+1}] \subset \mathcal{X}$  and  $[\underline{x}_{k+1}, \bar{x}_{k+1}] \cap \mathcal{X}_u = \emptyset$ . The constraints (15) enforce  $[\underline{x}_{k+1}, \bar{x}_{k+1}] \cap \mathcal{X}_u = \emptyset$  using integer variables according to

$$\begin{cases} \underline{x}_{k+1,j} \leq \bar{x}_{k+1,j} \leq \underline{x}_{u,j} & \text{if } \delta_{1,j}^u = 1, \delta_{2,j}^u = 0 \\ \bar{x}_{k+1,j} \geq \underline{x}_{k+1,j} \geq \bar{x}_{u,j} & \text{if } \delta_{1,j}^u = 0, \delta_{2,j}^u = 1 \\ \underline{x}_{u,j} \leq \bar{x}_{k+1,j} \leq \bar{x}, \underline{x} \leq \underline{x}_{k+1,j} \leq \bar{x}_{u,j} & \text{if } \delta_{1,j}^u = 0, \delta_{2,j}^u = 0 \end{cases},$$

where  $\bar{x}_{k+1,j}, \underline{x}_{k+1,j}, \bar{x}_{u,j}, \underline{x}_{u,j}$  are the  $j^{\text{th}}$  element of  $\bar{x}_{k+1}, \underline{x}_{k+1}, \bar{x}_u, \underline{x}_u$ , respectively. The integer constraints imply that there exists at least one dimension  $j$  where  $[\underline{x}_{k+1,j}, \bar{x}_{k+1,j}] \cap [\underline{x}_{u,j}, \bar{x}_{u,j}] = \emptyset$ . Subsequently, the hypercube  $[\underline{x}_{k+1}, \bar{x}_{k+1}]$  has zero overlaps with the unsafe subset  $[\underline{x}_u, \bar{x}_u]$ . Notably, in the case of a complex unsafe region  $\mathcal{X}_u$ , we can derive a union of hypercubes  $\cup_i \mathcal{X}_u^{(i)}$  as in (8c) that over-bounds  $\mathcal{X}_u$ . Thereafter, to ensure safety, we can formulate similar constraints (15) with each individual hypercube  $\mathcal{X}_u^{(i)}$  in the union. The proof is available in Appendix A.3.

### 3.4. Safe Tracking Control using MILP

The optimization objective in (5a) is designed to minimize the maximum distance between the points in the reachable set and the reference state  $x^r$ . Focusing on the case when  $p = 1$ , i.e., the cost is defined using  $\ell_1$  norm, we can introduce a vector of slack variables  $\lambda \in \mathbb{R}^{n_x}$ , and reformulate (5a) as

$$\text{argmin}_{\tilde{u}_k} \sum_{q=1}^{n_x} \lambda_q,$$

$$\text{subject to} \quad \lambda \geq 0, \quad -\lambda \leq \underline{x}_{k+1} - x^r \leq \lambda, \quad -\lambda \leq \bar{x}_{k+1} - x^r \leq \lambda, \quad (16)$$

where  $\lambda_q$  designates the  $q$ th element of vector  $\lambda$ . This objective function relies on the fact that the maximum distance, between a reference  $x^r$  and points in the hypercube  $[\underline{x}_{k+1}, \bar{x}_{k+1}]$ , is attained at the points located at the boundary of the hypercube. Then, the optimization problem (5) for tracking the reference state  $x^r$  safely can be rewritten into a MILP according to

**Robust Constrained Tracking Control Problem:**

$$\begin{aligned}
 & \underset{\substack{\tilde{u}_k, \delta^a, \delta^b, a_0, b_0, a_{k+1}, b_{k+1}, \underline{x}_{k+1}, \bar{x}_{k+1}, \delta_1^u, \delta_2^u, \lambda, \\ a_i, b_i, \hat{a}_i, \hat{b}_i, \delta_i^{--}, \delta_i^{+-}, \delta_i^{++}, i=1, \dots, \ell-1,}}{\text{argmin}} \sum_{q=1}^{n_x} \lambda_q, \\
 & \text{subject to: (9), (10), (11), (12), (13), (14), (15), (16).}
 \end{aligned} \tag{17}$$

We note that the number of decision variables in the MILP problem (17) scales linearly with the number of neurons in the NN. It also has the following property and the proof is presented in Appendix A. In the subsequent examples, we use the *YALMIP* toolbox (Lofberg (2004)) for MATLAB to solve the optimization (17).

**Proposition 4** Consider a NN-learned dynamical system defined by (1), (7) that takes control  $u_k$  and state  $x_k$  as inputs and yields  $\tilde{x}_{k+1}$  as a prediction of the next state  $x_{k+1}$  and satisfies the bounded additive error assumption in (2), (6a). We assume that  $x_k \in \mathcal{X}_s$  is unknown but belongs to a safe set  $\mathcal{X}_s = \mathcal{X} \setminus \mathcal{X}_u$  that is the complement set of the unsafe region  $\mathcal{X}_u$  given by (8c) in the state space  $\mathcal{X}$  defined by (8a). Suppose also that a measurement  $y_k$  of  $x_k$  is given that satisfies the assumptions in (3), (6b). If there exists a solution of the Problem (17) such that the corresponding  $\tilde{u}_k$  is in the admissible set  $\mathcal{U}$  defined by (8b), then for all actuator disturbances  $w_k^u$  in set  $\mathcal{W}_u$  defined by (6c), the actual control  $u_k$  subject to this additive disturbance  $w_k^u$  according to (4) renders the actual next state safe, i.e.,  $x_{k+1} \in \mathcal{X}_s$ .

#### 4. Obstacle Avoidance and Reachability-Guided RRT

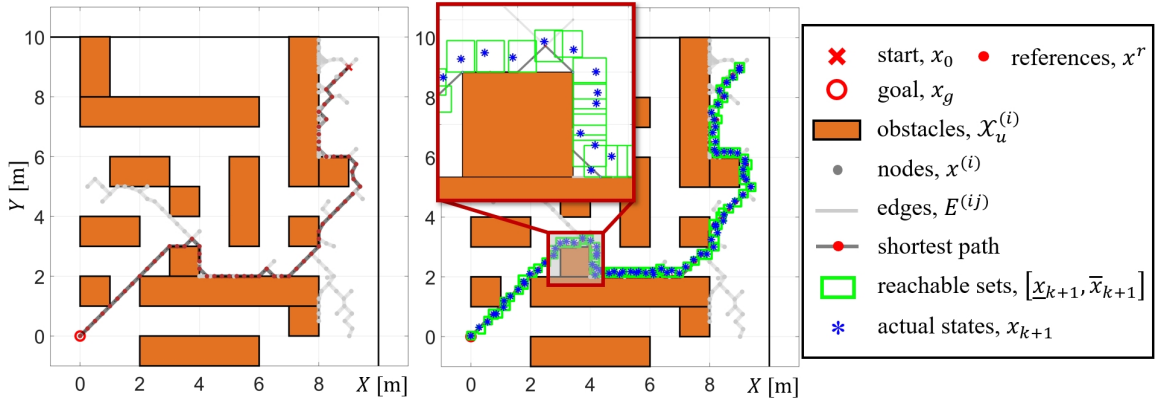


Figure 2: Schematic of obstacle avoidance using an omnidirectional robot: (Left) The reachability-guided RRT algorithm expands the tree from the start  $x_0$  to the goal  $x_g$  over the safe state space  $\mathcal{X}_s$ . Then, we use the Dijkstra planning algorithm to find a reference path (black lines with red dots) from  $x_0$  to  $x_g$  that has the shortest distance defined by  $\ell_1$  norm. (Middle) We use the proposed method in (17) to track the reference states (red dots). Our method can guarantee that the robot is collision-free under uncertainties, i.e., the unknown actual states in blue asterisks are in the safe set  $\mathcal{X}_s$ , even with most of the reference points located near the obstacles. A demonstration video is available at <https://xiaolisean.github.io/publication/2023-11-01-L4DC2024>.

We consider an omnidirectional robot as a mass point and use the following equation to represent its kinematics  $x_{k+1} = f(x_k, u_k) = x_k + u_k + w_k$ , where  $x_k \in \mathbb{R}^2$  is its coordinate in the  $X-Y$  plane and  $u_k \in \mathbb{R}^2$  is the displacement, and the value of the disturbance  $w_k \sim U(-\epsilon^x, \epsilon^x)$  are sampled



uniformly from the interval  $[-\epsilon^x, \epsilon^x]$ . We use the sets  $\mathcal{U} = \{[u_1 \ u_2]^T \in \mathbb{R}^2 : -0.25 \leq u_1, u_2 \leq -0.25\}$ ,  $\mathcal{X} = \{[x_1 \ x_2]^T \in \mathbb{R}^2 : -1 \leq x_1, x_2 \leq 10\}$  together with obstacles  $\mathcal{X}_u^{(i)}$  visualized in orange boxes in Figure 2. The NN is manually constructed and admits the following form

$$\tilde{x}_{k+1} = \begin{bmatrix} -I_{2 \times 2} & -I_{2 \times 2} \end{bmatrix} \text{ReLU} \left( \begin{bmatrix} I_{2 \times 2} & 0_{2 \times 2} \\ 0_{2 \times 2} & I_{2 \times 2} \end{bmatrix} \begin{bmatrix} x_k \\ u_k \end{bmatrix} + \begin{bmatrix} -50 \cdot \mathbb{1}_{2 \times 1} \\ -50 \cdot \mathbb{1}_{2 \times 1} \end{bmatrix} \right) + 100 \cdot \mathbb{1}_{2 \times 1},$$

which is equivalent to  $\tilde{x}_{k+1} = \tilde{f}(x_k, u_k) = x_k + u_k$  given  $x_k \in \mathcal{X}$  and  $u_k \in \mathcal{U}$ . Finally, the uncertainty bounds are set to  $\epsilon^x = \epsilon^u = \epsilon^y = [0.05, 0.05]^T$ . We develop a reachability-guided RRT planner similar to Shkolnik et al. (2009), combined with the Dijkstra algorithm, to generate a path of reference states  $x^r$ . Different from the classic RRT, the reachability-guided RRT incorporates dynamics as a constraint to extend the edges of the tree. This tree  $\mathcal{T}(\{x^{(i)}\}, \{E^{(ij)}\})$  comprises nodes  $x^{(i)} \in \mathcal{X}_s$  and directed edges  $E^{(ij)}$ . The edge  $E^{(ij)}$  connects node  $x^{(i)}$  to node  $x^{(j)}$  and implies that there exists a control  $u_k \in \mathcal{U}$  such that  $x^{(j)} = \tilde{f}(x^{(i)}, u_k) \in \mathcal{X}_s$ , i.e.,  $x^{(j)} \in \tilde{\mathcal{F}}(\{x^{(i)}\}, \mathcal{U}) \cap \mathcal{X}_s$ . As shown in Figure 2, the algorithm is initialized with an initial node  $x_0$  and is terminated if there exists a node  $x^{(i)} \in \mathcal{T}$  such that  $x_g \in \tilde{\mathcal{F}}(\{x^{(i)}\}, \mathcal{U})$ . At each time step, we take the first node  $x^{(i)}$  in the shortest path as the reference state  $x^r$  in (17). We solve the optimization (17) and apply the resulted control  $\tilde{u}_k$  to the actual dynamic model  $f$ . Then, we remove  $x^{(i)}$  from the path if  $x^{(i)} \in [\underline{x}_{k+1}, \bar{x}_{k+1}]$  and the navigation terminates when  $x_g \in [\underline{x}_{k+1}, \bar{x}_{k+1}]$ . As shown in Figure 2, after taking control  $\tilde{u}_k$ , the resulted next states  $x_{k+1}$  in blue asterisks are within the reachable set  $[\underline{x}_{k+1}, \bar{x}_{k+1}]$  in green boxes and the boxes  $[\underline{x}_{k+1}, \bar{x}_{k+1}]$  are collision-free which empirically validates the Proposition 4.

## 5. Vehicle Navigation and Set-theoretical Localization

As shown in Figure 3, we consider a front-wheel drive vehicle of width 2 m, and the length of the vehicle wheelbase is  $l = 5$  m. We adopt the vehicle kinematics model from Li et al. (2023) that admits the following form,

$$x_{k+1} = f(x_k, u_k) = \begin{bmatrix} p_{x,k} + v_k dt \cos \theta_k \cos \delta_k \\ p_{x,k} + v_k dt \sin \theta_k \cos \delta_k \\ \theta_k + v_k dt / l \sin \delta_k \end{bmatrix},$$

where  $x_k = [p_{x,k} \ p_{y,k} \ \theta_k]^T$  is the state vector,  $(p_{x,k}, p_{y,k})$  in meter is the coordinate of the center of the vehicle rear wheel axis, and  $\theta_k \in [-\pi, \pi]$  is the vehicle orientation;  $u_k = [v_k \ \delta_k]^T$  is the control vector,  $v_k$  in m/s is the vehicle longitudinal speed, and  $\delta_k$  in rad is the vehicle steering angle;  $dt = 0.1$  sec is the sampling period. We use the sets  $\mathcal{U} = \{u_k : v_k \in [2, 5], \delta_k \in [-0.6, 0.6]\}$ ,  $\mathcal{X} = \{x_k : p_{x,k}, p_{y,k} \in [-50, 50], \theta_k \in [-\pi, \pi]\}$  together with obstacles  $\mathcal{X}_u^{(i)}$  visualized in grey boxes in Figure 3. For the uncertainties, we assume the actuator disturbance  $\epsilon^u = [0.01 \text{ m/s}, 0.5 \text{ deg}]^T$ . We densely sample a dataset  $\mathcal{D} = \{(x_k^{(i)}, u_k^{(i)}, x_{k+1}^{(i)})\}_i$  from  $\mathcal{X} \times \mathcal{U}$  for NN training and quantifying the NN prediction error. We train an NN  $\tilde{f}$  using Stochastic Gradient Descent algorithm and dataset  $\mathcal{D}$  to minimize the mean-squared error  $\|x_{k+1}^{(i)} - \tilde{f}(x_k^{(i)}, u_k^{(i)})\|_2^2$ , and the prediction error is equal to  $\epsilon^x = [0.02 \text{ m}, 0.02 \text{ m}, 1.5 \text{ deg}]^T$ . We quantify the prediction error as the maximum value of the empirical absolute error, i.e.,

$$\epsilon^x = \max \left\{ \epsilon \in \mathbb{R}^3 : \epsilon = \left| x_{k+1}^{(i)} - \tilde{f}(x_k^{(i)}, u_k^{(i)}) \right|, (x_k^{(i)}, u_k^{(i)}, x_{k+1}^{(i)}) \in \mathcal{D} \right\},$$

and the function  $\max$  is applied element-wise. The theoretical properties of uncertainty-bound quantification from samples are discussed in Dean et al. (2020) and are not in the scope of this work.

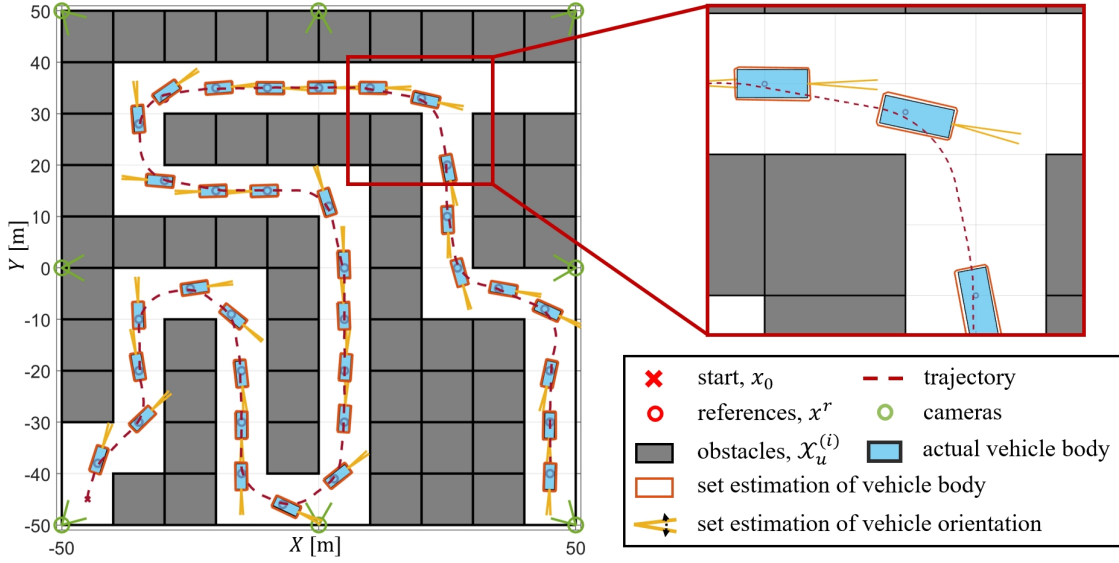


Figure 3: Schematic of navigating a vehicle through a maze with tracking controller (17) and with a set-theoretic localization algorithm. The zoom-in view, at the top-left, demonstrates that the set-theoretic localization algorithm provides estimations of the vehicle body and orientation that are guaranteed to contain the actual ones. The tracking controller (17) leverages this information, together with an NN-learned vehicle dynamics model, to avoid obstacles. A demonstration video is available at <https://xiaolisean.github.io/publication/2023-11-01-L4DC2024>.

At each time step  $k$ , we apply the set-theoretic localization algorithm presented in Li et al. (2023) to generate an uncertainty polygon  $P_{xy}$  that contains the actual vehicle position  $[p_{x,k}, p_{y,k}]^T$  and an uncertainty interval  $P_\theta$  that contains the actual vehicle orientation  $\theta_k$ , i.e.,  $[p_{x,k}, p_{y,k}]^T \in P_{xy}$  and  $\theta_k \in P_\theta$ . Subsequently, we can derive the smallest hypercube  $P$  that over-bound  $P_{xy} \times P_\theta$ , and the measurement error  $\epsilon^y$  is quantified as half of the sizes of  $P$ . The algorithm can also render a polytope estimation of the vehicle body as demonstrated in Figure 3. Then, akin to the process in Section 4, we solve the optimization problem (17) and use the resulting control to navigate the vehicle through the maze. As shown in Figure 3, we can also observe that the vehicle is collision-free, which is guaranteed formally by Proposition 4.

## 6. Conclusion and Future Work

In this paper, we developed an approach for robust reference tracking that leveraged a learned NN model to control the actual dynamics. We considered both bounded intrinsic and extrinsic uncertainties. We transcribed the resulting variable uncertainty set propagation through NN using a MILP. We provided formal proof that the proposed MILP can render the actual system state safe considering all possible actuator disturbance, measurement noise, and prediction error within their corresponding bounded sets. We test the proposed method in navigation and obstacle avoidance of omnidirectional robots and vehicles in simulations. Future works will include the investigation into methods to tighten the over-estimation by the hypercubes, and extension to ensure the recursive feasibility of the proposed MILP.

## References

- Anil Aswani, Humberto Gonzalez, S Shankar Sastry, and Claire Tomlin. Provably safe and robust learning-based model predictive control. *Automatica*, 49(5):1216–1226, 2013.
- Dan Barnes, Will Maddern, and Ingmar Posner. Find your own way: Weakly-supervised segmentation of path proposals for urban autonomy. In *2017 IEEE International Conference on Robotics and Automation (ICRA)*, pages 203–210. IEEE, 2017.
- Felix Berkenkamp, Riccardo Moriconi, Angela P Schoellig, and Andreas Krause. Safe learning of regions of attraction for uncertain, nonlinear systems with gaussian processes. In *Conference on Decision and Control*, pages 4661–4666. IEEE, 2016.
- Liyun Dai, Ting Gan, Bican Xia, and Naijun Zhan. Barrier certificates revisited. *Journal of Symbolic Computation*, 80:62–86, 2017.
- Sarah Dean and Benjamin Recht. Certainty equivalent perception-based control. In *Learning for Dynamics and Control*, pages 399–411. PMLR, 2021.
- Sarah Dean, Nikolai Matni, Benjamin Recht, and Vickie Ye. Robust guarantees for perception-based control. In *Learning for Dynamics and Control*, pages 350–360. PMLR, 2020.
- Sarah Dean, Andrew Taylor, Ryan Cosner, Benjamin Recht, and Aaron Ames. Guaranteeing safety of learned perception modules via measurement-robust control barrier functions. In *Conference on Robot Learning*, pages 654–670. PMLR, 2021.
- Yarin Gal and Zoubin Ghahramani. Dropout as a bayesian approximation: Representing model uncertainty in deep learning. In *international conference on machine learning*, pages 1050–1059. PMLR, 2016.
- Lukas Hewing, Kim P Wabersich, Marcel Menner, and Melanie N Zeilinger. Learning-based model predictive control: Toward safe learning in control. *Annual Review of Control, Robotics, and Autonomous Systems*, 3:269–296, 2020.
- Kurt Hornik, Maxwell Stinchcombe, and Halbert White. Multilayer feedforward networks are universal approximators. *Neural networks*, 2(5):359–366, 1989.
- Haimin Hu, Mahyar Fazlyab, Manfred Morari, and George J Pappas. Reach-sdp: Reachability analysis of closed-loop systems with neural network controllers via semidefinite programming. In *2020 59th IEEE Conference on Decision and Control (CDC)*, pages 5929–5934. IEEE, 2020.
- Balaji Lakshminarayanan, Alexander Pritzel, and Charles Blundell. Simple and scalable predictive uncertainty estimation using deep ensembles. *Advances in neural information processing systems*, 30, 2017.
- Yann LeCun, Yoshua Bengio, and Geoffrey Hinton. Deep learning. *nature*, 521(7553):436–444, 2015.
- Xiao Li, Yutong Li, Nan Li, Anouck Girard, and Ilya Kolmanovsky. Set-theoretic localization for mobile robots with infrastructure-based sensing. *Advanced Control for Applications: Engineering and Industrial Systems*, 5(1):e117, 2023.

- Johan Lofberg. Yalmip: A toolbox for modeling and optimization in matlab. In *2004 IEEE international conference on robotics and automation (IEEE Cat. No. 04CH37508)*, pages 284–289. IEEE, 2004.
- Alexander Shkolnik, Matthew Walter, and Russ Tedrake. Reachability-guided sampling for planning under differential constraints. In *2009 IEEE International Conference on Robotics and Automation*, pages 2859–2865. IEEE, 2009.
- Vincent Tjeng, Kai Xiao, and Russ Tedrake. Evaluating robustness of neural networks with mixed integer programming. *arXiv preprint arXiv:1711.07356*, 2017.
- Mukun Tong, Charles Dawson, and Chuchu Fan. Enforcing safety for vision-based controllers via control barrier functions and neural radiance fields. In *2023 IEEE International Conference on Robotics and Automation (ICRA)*, pages 10511–10517. IEEE, 2023.
- Li Wang, Dongkun Han, and Magnus Egerstedt. Permissive barrier certificates for safe stabilization using sum-of-squares. In *2018 Annual American Control Conference (ACC)*, pages 585–590. IEEE, 2018.
- Tianhao Wei and Changliu Liu. Safe control with neural network dynamic models. *arXiv preprint arXiv:2110.01110*, 2021.

## Appendix A. Formal Safety Guarantee

The proofs of Proposition 1, 2, 3 are presented in A.1, A.2, A.3, respectively. Subsequently, the hypercube defined by the lower and upper bounds  $\underline{x}_{k+1}, \bar{x}_{k+1}$ , as a result of the MILP problem (17), contains the actual state  $x_{k+1}$ , and the hypercube is within the safe set  $\mathcal{X}_s$ , i.e.,  $x_{k+1} \in [\underline{x}_{k+1}, \bar{x}_{k+1}] \subset \mathcal{X}_s$ . This proves Proposition 4.

### A.1. Input Constraints

**Proof** Based on assumption in (3) and  $x_k \in \mathcal{X}_s \subset \mathcal{X}$ , it's obvious that  $x_k \in \mathcal{X}_k = (y_k \ominus \mathcal{W}_y) \cap \mathcal{X}_s$  by the definition of Pontryagin difference, thereby we have  $x_k \in \mathcal{X}_k \subset (y_k \ominus \mathcal{W}_y) \cap \mathcal{X}$ . As defined in (9) together with the hypercube assumptions in (6b), (8a), the following statement can be proved

$$\forall x \in (y_k \ominus \mathcal{W}_y) \cap \mathcal{X}, \quad a_{0,1:n_x} = \max\{\underline{x}, y_k - \epsilon^y\} \leq x \leq \min\{\bar{x}, y_k + \epsilon^y\} = b_{0,1:n_x}.$$

Therefore, we can conclude that

$$x_k \in [a_{0,1:n_x}, b_{0,1:n_x}]. \quad (18)$$

Similarly, based on (4) and  $u_k \in \mathcal{U}$ , we can show that  $u_k \in \mathcal{U}_k$  and  $\max\{\underline{u}, \tilde{u}_k - \epsilon^u\} \leq u \leq \min\{\bar{u}, \tilde{u}_k + \epsilon^u\}$  for all  $u \in \mathcal{U}_k$ . Next, we need to show that the constraints (10) imply  $a_{0,(n_x+1):(n_x+n_u)} = \max\{\underline{u}, \tilde{u}_k - \epsilon^u\}$  and  $b_{0,(n_x+1):(n_x+n_u)} = \min\{\bar{u}, \tilde{u}_k + \epsilon^u\}$  from which we can conclude

$$u_k \in [a_{0,(n_x+1):(n_x+n_u)}, b_{0,(n_x+1):(n_x+n_u)}]. \quad (19)$$

If  $\delta_j^a = 1$ , the constraints (10) yield the following inequalities

$$\begin{cases} a_{0,j} \geq \underline{u}_j \\ a_{0,j} \geq \tilde{u}_{k,j} - \epsilon_j^u \\ a_{0,j} \leq \underline{u}_j \\ a_{0,j} \leq \tilde{u}_{k,j} - \epsilon_j^u + \max\{\epsilon_j^u, \bar{u}_j - \underline{u}_j - \epsilon_j^u\} \end{cases}$$

where the first three inequalities are equivalent to  $a_{0,j} = \underline{u}_j$ ,  $\underline{u}_j \geq \tilde{u}_{k,j} - \epsilon_j^u$ . In this case, we have  $a_{0,j} = \max\{\underline{u}_j, \tilde{u}_{k,j} - \epsilon_j^u\}$  and the fourth inequality is valid since  $\underline{u}_j \leq \tilde{u}_{k,j} \leq \bar{u}_j$  and  $a_{0,j} - \tilde{u}_{k,j} + \epsilon_j^u \leq \underline{u}_j - \underline{u}_j + \epsilon_j^u \leq \epsilon_j^u \leq \max\{\epsilon_j^u, \bar{u}_j - \underline{u}_j - \epsilon_j^u\}$ .

If  $\delta_j^a = 0$ , the constraints (10) produce the following inequalities

$$\begin{cases} a_{0,j} \geq \underline{u}_j \\ a_{0,j} \geq \tilde{u}_{k,j} - \epsilon_j^u \\ a_{0,j} \leq \tilde{u}_{k,j} - \epsilon_j^u \\ a_{0,j} \leq \underline{u}_j + \max\{\epsilon_j^u, \bar{u}_j - \underline{u}_j - \epsilon_j^u\} \end{cases}$$

where the first three inequalities are equivalent to  $a_{0,j} = \tilde{u}_{k,j} - \epsilon_j^u$ ,  $\tilde{u}_{k,j} - \epsilon_j^u \geq \underline{u}_j$ . Again, we can show  $a_{0,j} = \max\{\underline{u}_j, \tilde{u}_{k,j} - \epsilon_j^u\}$  and the fourth inequality is also feasible since  $a_{0,j} - \underline{u}_j = \tilde{u}_{k,j} - \epsilon_j^u - \underline{u}_j \leq \bar{u}_j - \epsilon_j^u - \underline{u}_j \leq \max\{\epsilon_j^u, \bar{u}_j - \underline{u}_j - \epsilon_j^u\}$ .

Hence, we can conclude that  $a_{0,j} = \max\{\underline{u}_j, \tilde{u}_{k,j} - \epsilon_j^u\}$  for  $j = (n_x + 1), \dots, (n_x + n_u)$  that is equivalent to  $a_{0,(n_x+1):(n_x+n_u)} = \max\{\underline{u}, \tilde{u}_k - \epsilon^u\}$  and the proof of  $b_{0,(n_x+1):(n_x+n_u)} = \min\{\bar{u}, \tilde{u}_k + \epsilon^u\}$  resembles the discussion above. Eventually, based on (18) and (19), the input  $z_0$  to the NN satisfies

$$z_0 = [x_k^T \ u_k^T]^T \in [a_0, b_0]. \quad (20)$$

■

## A.2. NN Structural Constraints

**Proof** We first provide proof of the following statement

$$\hat{z}_i = W^{(i)} z_{i-1} + b^{(i)} \in [\hat{a}_i, \hat{b}_i], \quad z_i = \max\{0, \hat{z}_i\} \in [a_i, b_i], \quad \text{given } z_{i-1} \in [a_{i-1}, b_{i-1}].$$

Then, from the results  $z_0 \in [a_0, b_0]$  in (20), we can inductively prove the same argument for  $i = 1, \dots, \ell - 1$ .

Given  $z_{i-1} \in [a_{i-1}, b_{i-1}]$ , the  $j^{th}$  element in  $\hat{z}_i$  is  $\hat{z}_{i,j} = w_j^{(i)} z_{i-1} + b_j^{(i)}$  where  $w_j^{(i)} = [w_1 \dots w_q \dots w_{n_{i-1}}]$  and satisfies the following inequalities

$$\begin{aligned} \sum_{q=1}^{n_{i-1}} (\llbracket w_q \geq 0 \rrbracket \cdot (w_q a_{i-1,q}) + \llbracket w_q < 0 \rrbracket \cdot (w_q b_{i-1,q})) \\ \leq \hat{z}_{i,j} - b_j^{(i)} \leq \\ \sum_{q=1}^{n_{i-1}} (\llbracket w_q \geq 0 \rrbracket \cdot (w_q b_{i-1,q}) + \llbracket w_q < 0 \rrbracket \cdot (w_q a_{i-1,q})), \end{aligned}$$

where the Iverson bracket  $\llbracket \cdot \rrbracket$  takes the value of 1 if the statement inside is true and 0 otherwise. We can derive the following equalities from the constraints in (11)

$$\begin{aligned} \hat{a}_{i,j} - b_j^{(i)} &= \sum_{q=1}^{n_{i-1}} (\llbracket w_q \geq 0 \rrbracket \cdot (w_q a_{i-1,q}) + \llbracket w_q < 0 \rrbracket \cdot (w_q b_{i-1,q})), \\ \hat{b}_{i,j} - b_j^{(i)} &= \sum_{q=1}^{n_{i-1}} (\llbracket w_q \geq 0 \rrbracket \cdot (w_q b_{i-1,q}) + \llbracket w_q < 0 \rrbracket \cdot (w_q a_{i-1,q})), \end{aligned}$$

which implies

$$\hat{z}_{i,j} \in [\hat{a}_{i,j}, \hat{b}_{i,j}], \quad j = 1, \dots, n_i. \quad (21)$$

Afterward, given  $\hat{z}_{i,j} \leq \hat{a}_{i,j} \leq \hat{z}_{i,j} \leq \hat{b}_{i,j} \leq \bar{z}_{i,j}$  in (11) and constraints in (12), we need to prove  $a_{i,j} \leq z_{i,j} \leq b_{i,j}$ . If  $\delta_{i,j}^- = 1$ , the constraints in (12) are reduced to

$$\begin{cases} b_{i,j} \geq a_{i,j} \geq 0 \\ \hat{a}_{i,j} \leq a_{i,j} \leq 0 \\ \hat{b}_{i,j} \leq b_{i,j} \leq 0 \\ a_{i,j} \leq \hat{a}_{i,j} - \hat{z}_{i,j} \\ b_{i,j} \leq \hat{b}_{i,j} - \hat{z}_{i,j} \end{cases}.$$

The first three inequalities are equivalent to  $a_{i,j} = b_{i,j} = 0$ ,  $\hat{a}_{i,j} \leq 0$ ,  $\hat{b}_{i,j} \leq 0$  which induce  $\hat{z}_{i,j} \leq \hat{b}_{i,j} \leq 0$  and  $z_{i,j} = \max\{0, \hat{z}_{i,j}\} = 0$ , thereby we have  $0 = a_{i,j} \leq z_{i,j} \leq b_{i,j} = 0$ . Meanwhile, the last two inequalities hold since  $\hat{z}_{i,j} \leq \hat{a}_{i,j} \leq \hat{z}_{i,j} \leq \hat{b}_{i,j} \leq \bar{z}_{i,j}$ .

If  $\delta_{i,j}^{++} = 1$ , the constraints in (12) are reduced to

$$\begin{cases} b_{i,j} \geq a_{i,j} \geq 0 \\ \hat{a}_{i,j} \leq a_{i,j} \leq 0 \\ \hat{b}_{i,j} \leq b_{i,j} \leq \hat{b}_{i,j} \\ a_{i,j} \leq \hat{a}_{i,j} - \hat{z}_{i,j} \\ b_{i,j} \leq \bar{z}_{i,j} \end{cases}.$$



The first three inequalities imply that  $a_{i,j} = 0$ ,  $\hat{a}_{i,j} \leq 0$  and  $b_{i,j} = \hat{b}_{i,j}$ ,  $\hat{b}_{i,j} \geq 0$  from which we can show that  $0 \leq z_{i,j} \leq \hat{b}_{i,j}$ . Thus, we have  $a_{i,j} = 0 \leq z_{i,j} \leq \hat{b}_{i,j} = b_{i,j}$  and the last two inequalities are also feasible.

If  $\delta_{i,j}^{++} = 1$ , the constraints in (12) are reduced to

$$\begin{cases} b_{i,j} \geq a_{i,j} \geq 0 \\ \hat{a}_{i,j} \leq a_{i,j} \leq \hat{a}_{i,j} \\ \hat{b}_{i,j} \leq b_{i,j} \leq \hat{b}_{i,j} \\ a_{i,j} \leq \hat{z}_{i,j} \\ b_{i,j} \leq \hat{z}_{i,j} \end{cases}.$$

The first three inequalities imply that  $a_{i,j} = \hat{a}_{i,j}$ ,  $\hat{a}_{i,j} \geq 0$  and  $b_{i,j} = \hat{b}_{i,j}$ ,  $\hat{b}_{i,j} \geq 0$  from which we can show  $\hat{a}_{i,j} \leq z_{i,j} \leq \hat{b}_{i,j}$ . Thus, we have  $a_{i,j} = \hat{a}_{i,j} \leq z_{i,j} \leq \hat{b}_{i,j} = b_{i,j}$  and the last two inequalities are valid. To this end, we have proven that

$$z_{i,j} \in [a_{i,j}, b_{i,j}], \quad j = 1, \dots, n_i. \quad (22)$$

Indeed, as discussed at the beginning of this section, we can show that

$$\hat{z}_i \in [\hat{a}_i, \hat{b}_i], \quad z_i \in [a_i, b_i], \quad i = 1, \dots, \ell - 1 \quad (23)$$

with (20). Identical to the proof of (21), given  $z_{\ell-1} \in [a_{\ell-1}, b_{\ell-1}]$  in (23), constraints in (13) and  $\tilde{x}_{k+1} = W^{(\ell)} z_{\ell-1} + b^{(\ell)}$  in (1), we can demonstrate that

$$\tilde{x}_{k+1} \in \tilde{\mathcal{F}}(\mathcal{X}_k, \mathcal{U}_k) \subseteq [a_{k+1}, b_{k+1}]. \quad (24)$$

■

### A.3. Output Constraints

**Proof** With the assumptions in (2) and (6a), we can show  $x_{k+1} \in [a_{k+1}, b_{k+1}] \oplus \mathcal{W}_x$  which can be further derived to

$$x_{k+1} \in [\underline{x}_{k+1}, \bar{x}_{k+1}] \subset \mathcal{X}, \quad (25)$$

based on the constraints in (14). Meanwhile, the constraints in (15) are equivalent to the following statement

$$\exists j \in \{1, \dots, n_x\}, \text{ s.t. } \delta_{1,j}^u = 1 \text{ or } \delta_{2,j}^u = 1.$$

In the sequel, we show that  $[\underline{x}_{k+1}, \bar{x}_{k+1}] \cap \mathcal{X}_u = \emptyset$  with constraints in (15) if  $\delta_{1,j}^u = 1$  which the proof resembles in case of  $\delta_{2,j}^u = 1$ . If  $\delta_{1,j}^u = 1$ , the constraints in (15) can be reformulated into

$$\underline{x}_j \leq \underline{x}_{k+1,j} \leq \bar{x}_{k+1,j} \leq \underline{x}_{u,j}.$$

Suppose  $[\underline{x}_{k+1}, \bar{x}_{k+1}] \cap \mathcal{X}_u \neq \emptyset$ , therefore there exists  $x^* = [x_1^* \cdots x_j^* \cdots x_{n_x}^*]^T \in \mathbb{R}^{n_x}$  such that  $x^* \in [\underline{x}_{k+1}, \bar{x}_{k+1}] \cap \mathcal{X}_u$ . Then, for some index  $j$  and  $1 \leq j \leq n_x$ , we have  $\underline{x}_{u,j} \leq x_j^* \leq \bar{x}_{u,j}$  and  $\underline{x}_{k+1,j} \leq x_j^* \leq \bar{x}_{k+1,j}$  which violates  $\bar{x}_{k+1,j} \leq \underline{x}_{u,j}$ . By contradiction, the following is true

$$[\underline{x}_{k+1}, \bar{x}_{k+1}] \cap \mathcal{X}_u = \emptyset. \quad (26)$$

With equations (25) and (26), we demonstrate that  $x_{k+1} \in \mathcal{F}(\mathcal{X}_k, \mathcal{U}_k) \subseteq [\underline{x}_{k+1}, \bar{x}_{k+1}] \subset \mathcal{X}_s$  which complete the proof for Proposition 3. ■